

ON THE IMPACT OF RECONFIGURABLE ANTENNA ARRAYS IN COGNITIVE RADIO

Akbar M. Sayeed*

University of Wisconsin-Madison
Dept. of Electrical and Computer Engr.
Madison, WI 53706, USA

Vasanthan Raghavan

University of Illinois at Urbana-Champaign
Dept. of Electrical and Computer Engr.
Urbana, IL 61801, USA

ABSTRACT

Technological advances in radio-frequency (RF) front-ends, such as reconfigurable antenna arrays, afford a new “hardware” dimension for dynamic spectrum access in cognitive wireless networks. In this paper, we study the impact of reconfigurable antenna arrays on maximizing the spectral efficiency of multiple input multiple output (MIMO) wireless communication links. Physical wireless channels exhibit spatial correlation and there is growing experimental evidence that sparse multipath is a key source of such correlation. We propose a model for sparse multipath channels and show that sparsity affords a new dimension over which MIMO capacity can be optimized: the distribution or configuration of the sparse statistically independent degrees of freedom (DoF) in the available spatial signal space dimensions. We provide an explicit characterization of the optimal capacity-maximizing channel configurations as a function of the operating SNR. We then develop a framework for realizing the optimal channel configuration at any SNR by *systematically* adapting the antenna spacings at the transmitter and the receiver. In contrast to a fixed-array MIMO system in which the multiplexing gain is lost at low SNRs, such adaptively reconfigurable MIMO systems deliver the maximum multiplexing gain at all SNRs. Surprisingly, three canonical array configurations are sufficient for near-optimum performance over the entire SNR range. Numerical results based on a realistic physical model are presented and implications of this work for cognitive radio and dynamic spectrum access are discussed.

Index Terms— Reconfigurable MIMO systems, sparse multipath, capacity, spectral efficiency

1. INTRODUCTION

With the inevitable trend towards proliferation of wireless devices, there is a growing need for developing new theory and methods for harnessing the potential of emerging wireless technology for spectral efficiency and interference management. Several recent lines of research address this multi-faceted challenge from different dimensions, including software-defined radio and cognitive wireless systems, waveform diversity techniques, and cross-layer techniques for dynamic spectrum management. However, most of these approaches implicitly assume communication devices with fixed radio-frequency (RF) front-ends and focus on system optimization at a “software” or algorithmic level.

Advances in reconfigurable RF front-ends, particularly reconfigurable antenna arrays, afford a new “hardware” dimension for optimizing the performance of wireless communication systems by adapting the array configuration to changes in the communication environment. However, theory and methods for maximal utilization

of such new wireless devices are still in their infancy. While the intense research on multiple input multiple output (MIMO) wireless communication systems was pioneered by initial results in rich multipath environments, there is growing evidence that physical wireless channels exhibit a *sparse* structure even at relatively small antenna dimensions. Recent studies also indicate that reducing the antenna spacings in such correlated environments can actually increase capacity in the low-SNR regime. Thus, understanding the impact of reconfigurable antenna arrays on MIMO capacity, and developing strategies for sensing and adapting to the environment, is of significant theoretical and practical interest.

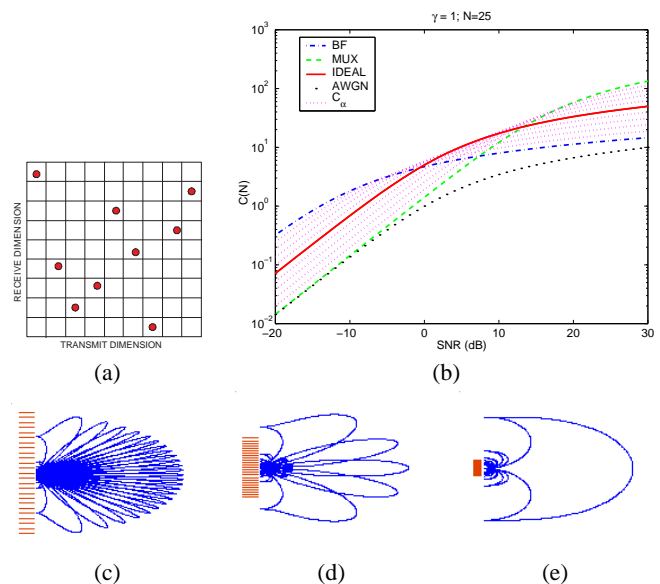


Fig. 1. (a) A sparse 9×9 virtual channel matrix. (b) Capacity versus SNR for different channel configurations for $D = N = 25$. (c)-(e): Virtual beam patterns for $N = 25$ and different spacings; (c) large spacing; (d) medium spacing; (e) small spacing.

In this paper, we propose a framework for maximizing the capacity of MIMO wireless links in sparse multipath by systematically adapting the array configurations at the transmitter and the receiver. We focus on uniform linear arrays (ULAs) of antennas and propose a model for sparse multipath channels using the virtual channel representation [1] that provides an accurate and analytically tractable model for physical multipath channels. Let \mathbf{H}_v denote an $N \times N$ virtual channel matrix representing N antennas at the transmitter and the receiver. The dominant non-vanishing entries of \mathbf{H}_v reveal the statistically independent degrees of freedom (DoF), D , in the channel which also represent the number of resolvable paths in the scat-

*This work was partly supported by the NSF under grant #CCF-0431088.

tering environment. In sparse channels, $D < N^2$, as illustrated in Fig. 1(a), and thus sparse channels afford a new dimension over which capacity can be optimized: the distribution (or configuration) of the D DoF in the available N^2 dimensions in \mathbf{H}_v . For a given N and D , we introduce a family of channel configurations described by two parameters (p, q) that are constrained as $D = pq$; p represents the multiplexing gain (the number of parallel channels) and $q = D/p$ reflects the DoF per parallel channel. The capacity of all configurations is accurately approximated by

$$C(N, \rho, D, p) \approx p \log(1 + \rho D/p^2) \quad (1)$$

where ρ denotes the transmit SNR and $\rho D/p^2 = \rho q/p = \rho_{rx}$ denotes the received SNR per parallel channel. The above formula reveals a fundamental new tradeoff in sparse channels between the multiplexing gain (MG) and ρ_{rx} that governs channel capacity: increasing p comes at the cost of ρ_{rx} and vice versa. This is illustrated in Fig. 1(b) where the capacity curves represent different values of p . For any ρ , there is an optimal channel configuration (value of p) that optimizes the MG- ρ_{rx} tradeoff and yields the highest capacity.

The optimal channel configuration at any SNR can be realized in practice by *systematically* adapting the antenna spacings at the transmitter (Tx) and receiver (Rx). Surprisingly, three canonical array configurations are sufficient for near-optimum performance over the entire SNR range. The multiplexing (MUX) configuration ($p = p_{max} = N$) in Fig. 1(b) is optimal at high SNR, $\rho > \rho_{high}$, and is realized by large spacings at both ends, illustrated in Fig. 1(c). The beamforming (BF) configuration ($p = p_{min} = 1$) is optimal at low SNR, $\rho < \rho_{low}$, and is realized by closely spaced antennas at the Tx (Fig. 1(e)) and large spacing at the Rx (Fig. 1(c)). The IDEAL configuration ($p = p_{id} = \sqrt{N}$) is a robust choice for $\rho \in (\rho_{low}, \rho_{high})$ and is realized by medium spacings at the Tx and the Rx (Fig. 1(d)). Thus, maximum multiplexing gain is achieved over the entire SNR range via the three canonical configurations. We illustrate our results with numerical simulations based on an accurate physical model, and provide a discussion of the potential of reconfigurable MIMO transceivers in cognitive radio and dynamic spectrum access.

2. PHYSICAL AND VIRTUAL MODELING OF MULTIPATH CHANNELS

We consider a single-user MIMO system with ULA's of N transmit and N receive antennas. The transmitted signal \mathbf{s} and the received signal \mathbf{x} are related by $\mathbf{x} = \mathbf{H}\mathbf{s} + \mathbf{n}$ where \mathbf{H} is the $N \times N$ MIMO channel matrix and \mathbf{n} is the AWGN at the receiver. A physical multipath channel can be accurately modeled as

$$\mathbf{H} = N \sum_{\ell=1}^L \beta_{\ell} \mathbf{a}_r(\theta_{r,\ell}) \mathbf{a}_t^H(\theta_{t,\ell}) \quad (2)$$

where the transmitter and receiver arrays are coupled through L propagation paths with complex path gains $\{\beta_{\ell}\}$, Angles of Departure (AoD) $\{\theta_{t,\ell}\}$ and Angles of Arrival (AoA) $\{\theta_{r,\ell}\}$. In (2), $\mathbf{a}_r(\theta_r)$ and $\mathbf{a}_t(\theta_t)$ denote the receiver response and transmitter steering vectors for receiving/transmitting in the normalized direction θ_r/θ_t , where θ is related to the physical angle (in the plane of the arrays) $\phi \in [-\pi/2, \pi/2]$ as $\theta = d \sin(\phi)/\lambda$, d is the antenna spacing and λ is the wavelength of propagation. Both $\mathbf{a}_r(\theta_r)$ and $\mathbf{a}_t(\theta_t)$ are periodic in θ with period 1 [1], and are also unit-norm and the factor N in (2) reflects this normalization.

The *virtual MIMO channel representation* [1] characterizes a physical channel via coupling between spatial beams in fixed virtual

transmit and receive directions

$$\mathbf{H} = \sum_{m=1}^{N_r} \sum_{n=1}^{N_t} H_v(m, n) \mathbf{a}_r(\tilde{\theta}_{r,m}) \mathbf{a}_t^H(\tilde{\theta}_{t,n}) = \mathbf{A}_r \mathbf{H}_v \mathbf{A}_t^H \quad (3)$$

where $\{\tilde{\theta}_{r,m} = \frac{m}{N_r}\}$ and $\{\tilde{\theta}_{t,n} = \frac{n}{N_t}\}$ are fixed virtual receive and transmit angles that uniformly sample the unit square in the beamspace, $(\theta_r, \theta_t) \in [-1/2, 1/2] \times [-1/2, 1/2]$, and result in unitary (DFT) matrices \mathbf{A}_t and \mathbf{A}_r . Thus, \mathbf{H} and \mathbf{H}_v are unitarily equivalent: $\mathbf{H}_v = \mathbf{A}_r^H \mathbf{H} \mathbf{A}_t$. The virtual representation is linear and is characterized by the matrix \mathbf{H}_v .

A key property of the virtual representation is that it induces a partitioning of paths in (2) [1]: *distinct* $\mathbf{H}_v(m, n)$'s are associated with approximately *disjoint* sets of paths whose AoA's and AoD's lie within the intersection of the n -th transmit and m -th receive beam. It follows that $\{\mathbf{H}_v(m, n)\}$ are approximately independent due to the independence of path gains.¹ We will assume that the virtual coefficients are exactly independent zero-mean Gaussian random variables (Rayleigh fading). Thus, the statistics of \mathbf{H} are characterized by the *virtual channel power matrix* Ψ : $\Psi(m, n) = E[|\mathbf{H}_v(m, n)|^2]$. The matrices \mathbf{A}_r and \mathbf{A}_t constitute the matrices of eigenvectors for the transmit and receive covariance matrices, respectively: $E[\mathbf{H}^H \mathbf{H}] = \mathbf{A}_t \mathbf{\Lambda}_t \mathbf{A}_t^H$ and $E[\mathbf{H} \mathbf{H}^H] = \mathbf{A}_r \mathbf{\Lambda}_r \mathbf{A}_r^H$, where $\mathbf{\Lambda}_t = E[\mathbf{H}_v^H \mathbf{H}_v]$ and $\mathbf{\Lambda}_r = E[\mathbf{H}_v \mathbf{H}_v^H]$ are the diagonal matrices of transmit and receive eigenvalues. Ψ reflects the *joint* distribution of channel power as a function of transmit and receive virtual angles. $\mathbf{\Lambda}_t$ and $\mathbf{\Lambda}_r$ serve as the corresponding *marginal* distributions: $\mathbf{\Lambda}_r(m) = \sum_n \Psi(m, n)$ and $\mathbf{\Lambda}_t(n) = \sum_m \Psi(m, n)$.

Measurement studies have shown that the dominant virtual coefficients tend to be *sparse* (see, e.g., [2]) even for relatively small $N \sim 8$. We abstract this concept in the following definition.

Definition 1 (Sparse Virtual Channels) *An $N \times N$ \mathbf{H}_v is sparse if it contains $D < N^2$ non-vanishing coefficients. We assume that each non-vanishing $\mathbf{H}_v(m, n)$ is $\mathcal{CN}(0, 1)$ reflecting the power contributed by the unresolvable paths associated with it. D reflects the statistically independent DoF in the channel and also the total channel power $\rho_c(N) = E[\text{tr}(\mathbf{H}_v \mathbf{H}_v^H)] = N^2 \sum_{\ell=1}^L E|\beta_{\ell}|^2 = D$. It is convenient to model a sparse \mathbf{H}_v through a mask matrix \mathbf{M}*

$$\mathbf{H}_v = \mathbf{M} \odot \mathbf{H}_{iid} \quad (4)$$

where \odot denotes element-wise product, \mathbf{H}_{iid} is an i.i.d. matrix with $\mathcal{CN}(0, 1)$ entries, and \mathbf{M} has D non-zero (unit) entries.

The coherent ergodic capacity of a MIMO channel, assuming knowledge of \mathbf{H} at the receiver, is given by

$$C(N, \rho) = \max_{\text{Tr}(\mathbf{Q}_v) \leq \rho} E_{\mathbf{H}_v} \left[\log \det \left(\mathbf{I} + \mathbf{H}_v \mathbf{Q}_v \mathbf{H}_v^H \right) \right] \quad (5)$$

where ρ is the transmit SNR, and $\mathbf{Q}_v = E[\mathbf{s}_v \mathbf{s}_v^H]$ is the covariance matrix of the (optimal) Gaussian input; $\mathbf{s}_v = \mathbf{A}_t^H \mathbf{s}$. It is shown in [3] that the capacity-maximizing $\mathbf{Q}_{v,opt}$ is diagonal. Furthermore, for general correlated channels, $\mathbf{Q}_{v,opt}$ is full-rank at high SNR's, whereas it is rank-1 at low SNR's. For an \mathbf{H}_v defined by a mask \mathbf{M} in (4) we denote the capacity by $C(N, \rho, \mathbf{M})$.

3. CAPACITY-MAXIMIZING CHANNEL CONFIGURATIONS

In this section, we review the theory behind our approach. We state the results without proof; the readers are referred to [4] for details.

¹This property has been validated with experimental measurements [2].

The capacity of a sparse channel depends on three fundamental quantities: 1) the transmit SNR ρ , 2) the number of DoF, $D < N^2$, and 3) the distribution of the D DoF in the available N^2 dimensions in \mathbf{H}_v . For any ρ there is an optimal channel configuration, characterized by an \mathbf{M}_{opt} , that yields the highest capacity at that ρ .

Definition 2 (Optimal Channel Configuration) Let $\mathcal{M}(D)$ denote the set of all $N \times N$ mask matrices with D non-zero (unit) entries. For any ρ , the optimal MIMO capacity is defined as

$$C_{opt}(N, D, \rho) = \max_{\mathbf{M} \in \mathcal{M}(D)} C(N, \rho, \mathbf{M}) \quad (6)$$

and an \mathbf{M}_{opt} that achieves $C_{opt}(N, D, \rho)$ defines the optimal channel configuration at that ρ .

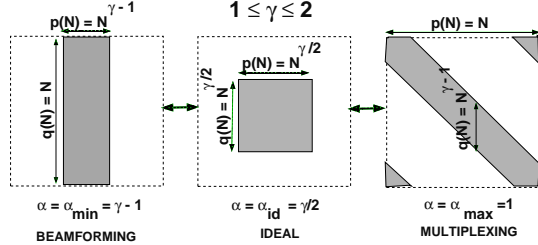


Fig. 2. A family of mask matrices. $\gamma \in [1, 2]$.

\mathbf{M}_{opt} is not unique in general. In [4] we present an explicit family of mask matrices, reflecting different configurations of the D DoF, to characterize the \mathbf{M}_{opt} for any given ρ . The family of mask matrices is defined by two parameters (p, q) such that $D = pq$. The parameter p reflects the multiplexing gain (number of parallel channels) afforded by the configuration and q reflects the DoF per parallel channel. For $D = N^\alpha$, $\alpha \in [\alpha_{min}, \alpha_{max}]$ where $\alpha_{min} = \max(\gamma - 1, 0)$ and $\alpha_{max} = \min(\gamma, 1)$, and $q = D/p$. The mask matrices are illustrated in Fig. 2 for $\gamma \in [1, 2]$. We next summarize the properties of the mask matrices relevant to this paper.

Proposition 1 For a given $D = N^\alpha$, $\alpha \in [0, 2]$, and any $p = N^\alpha$, $\alpha \in [\alpha_{min}, \alpha_{max}]$, the mask matrix $\mathbf{M}(D, p)$ is an $N \times N$ matrix whose non-zero entries are contained in a sub-matrix of size $r \times p$, $r = \max(q, p)$, consisting of p non-zero columns, and q non-zero (unit) entries in each column. The corresponding $r \times p$ virtual sub-matrices $\tilde{\mathbf{H}}_v$ defined by (4) satisfy $\rho_c = D$ and their transmit and receive covariance matrices are given by

$$\tilde{\Lambda}_t = E[\tilde{\mathbf{H}}_v^H \tilde{\mathbf{H}}_v] = \frac{D}{p} \mathbf{I}_p, \quad \tilde{\Lambda}_r = E[\tilde{\mathbf{H}}_v \tilde{\mathbf{H}}_v^H] = \frac{D}{r} \mathbf{I}_r \quad (7)$$

Remark 1 Since the non-zero transmit eigenvalues are identical, the optimal input allocates power uniformly to the corresponding transmit dimensions, $\tilde{\mathbf{Q}}_{v,opt} = \frac{D}{p} \mathbf{I}_p$, and no power to others.

The channel capacity for any $\mathbf{M}(D, p)$, $C(N, \rho, \mathbf{M}(D, p))$, is given by (1) which was derived for large N but yields accurate estimates even for relatively small N . The following theorem characterizes the optimal channel configuration.

Theorem 1 For a given ρ , the optimal channel configuration is characterized by $\mathbf{M}(D, p_{opt}) \leftrightarrow p_{opt}$ where

$$p_{opt} \approx \begin{cases} p_{min} & , \quad \rho < \rho_{low} \\ \frac{\sqrt{\rho D}}{2} & , \quad \rho \in [\rho_{low}, \rho_{high}] \\ p_{max} & , \quad \rho > \rho_{high} \end{cases} \quad (8)$$

and $C_{opt}(N, D, \rho) = C(N, \rho, \mathbf{M}(D, p_{opt}))$. In (8), $p_{min} = N^{\alpha_{min}}$, $p_{max} = N^{\alpha_{max}}$, $\rho_{low} \approx 4p_{min}^2/D$ and $\rho_{high} \approx 4p_{max}^2/D$.

Remark 2 (Multiplexing gain versus Received SNR Tradeoff) As noted earlier, (1) reveals a multiplexing gain (MG) versus received SNR tradeoff that governs capacity: increasing the MG (p) comes at the cost of a reduction in $\rho_{rx} = \rho D/p^2$ and vice versa. The ratio $\rho_{high}/\rho_{low} = (p_{max}/p_{min})^2$ attains its largest value, N^2 , for $D = N$ ($\gamma = 1$), whereas it achieves its minimum value of unity for $D = 1$ ($\gamma = 0$) or $D = N^2$ ($\gamma = 2$). Thus, the MG- ρ_{rx} tradeoff does not exist for the extreme cases of highly correlated ($D = 1$) and i.i.d. ($D = N^2$) channels. On the other hand, the impact of the tradeoff on capacity is highest for $D = N$.

4. CAPACITY-MAXIMIZING ARRAY CONFIGURATIONS

In this section we present a systematic approach for maximizing MIMO capacity in sparse multipath environments by adapting the antenna spacings at the transmitter (d_t) and receiver (d_r). We focus on the $D = N$ case (see Rem. 2). We first define the notion of randomly sparse physical channels.

Definition 3 (Randomly Sparse Physical Channels) For a given N , a class $\mathcal{H}(D)$ of channels is said to be randomly sparse with D DoF if it contains $L = D < N^2$ resolvable paths that are randomly distributed over the maximum angular spreads for sufficiently large antenna spacings $d_{t,max}$ and $d_{r,max}$; that is, $(\theta_{r,\ell}, \theta_{t,\ell}) \in [-1/2, 1/2] \times [-1/2, 1/2]$ in (2). We assume that the path gains are independent and satisfy $N^2 \beta_\ell \sim \mathcal{CN}(0, 1)$.

Maximum antenna spacings serve as the anchor point for relating to the theory in Sec. 3 and correspond to the MUX configuration ($p = p_{max} = N$): $(d_{t,max}, d_{r,max}) \leftrightarrow p_{max}$. The next result describes the required spacings to create a channel configuration whose statistics match those induced by $\mathbf{M}(D, p)$ for any p in Prop. 1.

Proposition 2 Consider the class of randomly sparse channels with $D = N$. For any p , $1 \leq p \leq N$, define the antennas spacings

$$d_t = \frac{p}{N} d_{t,max}, \quad d_r = \frac{r}{N} d_{r,max} \quad (9)$$

where $r = \max(q, p)$ and $q = D/p$. Then, for each p , the non-vanishing entries of the resulting $\tilde{\mathbf{H}}_v$ are approximately contained within an $r \times p$ sub-matrix $\tilde{\mathbf{H}}_v$ with power matrix $\tilde{\Psi} = \frac{D}{p} \mathbf{1}_{r \times p}$. Furthermore, the transmit and receive covariance matrices, $\tilde{\Lambda}_t$ and $\tilde{\Lambda}_r$, of $\tilde{\mathbf{H}}_v$ match those generated by $\mathbf{M}(D, p)$ in Prop. 1.

Proof (sketch): The D randomly distributed paths cover maximum angular spreads (AS's) in the θ domain at the maximum spacings. Since $\theta = d \sin(\phi)/\lambda$, where ϕ is the physical path angle (which remains unchanged), the d_t and d_r in (9) result in smaller AS's in the θ domain: $\theta_{t,\ell} \in [-p/2N, p/2N]$ at the transmitter and $\theta_{r,\ell} \in [-r/2N, r/2N]$ at the receiver. Since the spacing between virtual angles is $\Delta\theta = 1/N$, only p virtual transmit angles and r virtual receive angles lie within the reduced AS's. Thus, the non-zero entries in $\tilde{\mathbf{H}}_v$ are contained in a sub-matrix $\tilde{\mathbf{H}}_v$ of size $r \times p$. The channel power $\rho_c = D$ is uniformly distributed so that $E[|\tilde{\mathbf{H}}_v(m, n)|^2] = \frac{D}{rp}$, $\tilde{\Lambda}_r = (D/r) \mathbf{I}_r$ and $\tilde{\Lambda}_t = q \mathbf{I}_p$, where the expectation is over the statistics of the D non-vanishing coefficients as well as their random locations. The proposition follows by comparison with Prop. 1. \square

Prop. 2 implies that for randomly sparse channels the $\tilde{\mathbf{H}}_v$ generated by adapting antenna spacings has identical statistics (marginal and joint) to those generated by $\mathbf{M}(D, p)$ in Prop. 1 for $p \leq q$, but

only the marginal statistics are matched for $p > q$. Thus, the actual capacity may deviate a little from (1) for $p > q$ especially at high SNR's. With this qualification, we have the following result.

Theorem 2 *In randomly sparse physical channels, the optimal channel configuration for any transmit SNR, ρ , can be created by choosing $d_{r,opt}$ and $d_{t,opt}$ in (9) corresponding to p_{opt} in (8).*

Remark 3 (Three Canonical Array Configurations) *Three configurations are highlighted in Fig. 1 for $N=D=25$: MUX – $\mathbf{H}_{v,mux} \leftrightarrow p_{mux} = N \leftrightarrow d_{t,mux} = d_{r,mux} = d_{max}$ (Fig. 1(c)); BF – $\mathbf{H}_{v,bf} \leftrightarrow p_{bf} = 1 \leftrightarrow d_{t,bf} = d_{t,mux}/N$ (Fig. 1(e)) and $d_{r,bf} = d_{r,mux}$ (Fig. 1(c)); and IDEAL – $\mathbf{H}_{v,id} \leftrightarrow p_{id} = \sqrt{N} \leftrightarrow d_{t,id} = d_{r,mux}/\sqrt{N}$ (Fig. 1(d)). The BF and MUX configurations are optimum for $\rho < \rho_{low}$ and $\rho > \rho_{high}$, respectively. The IDEAL configuration is a good approximation to the optimum for $\rho \in (\rho_{low}, \rho_{high})$. These three array configurations suffice for maximizing capacity over the entire SNR range in practice.*

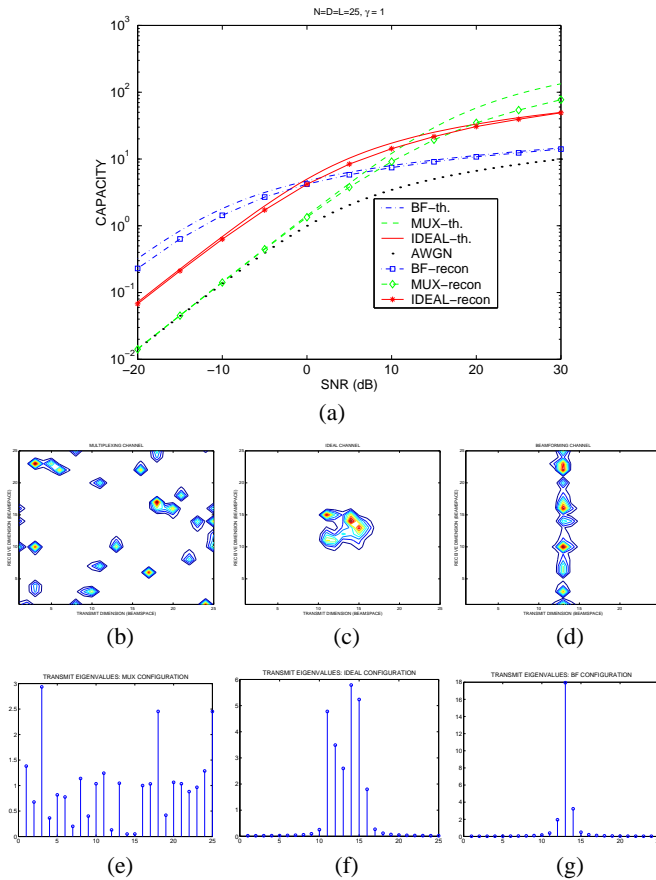


Fig. 3. (a): Simulated and theoretical capacities for the three canonical array configurations. (b)-(d): Contour plots of Ψ ; (b) Ψ_{mux} , (c) Ψ_{id} , (d) Ψ_{bf} . (e)-(g): Transmit eigenvalues; (e) $\Lambda_{t,mux}$, (f) $\Lambda_{t,id}$, (g) $\Lambda_{t,bf}$.

We now present a numerical example to illustrate the creation of $\mathbf{H}_{v,mux}$, $\mathbf{H}_{v,id}$, and $\mathbf{H}_{v,bf}$ by adapting the antenna spacings as in Prop. 2 and Rem. 3. We consider $N = D = 25$ and first generate the physical AoA's and AoD's, $(\phi_{t,\ell}, \phi_{r,\ell}) \in [-\pi/2, \pi/2]^2$, for $L = 25$ paths that are randomly distributed over the maximum angular spreads at $d_{t,mux} = d_{r,mux} = d_{max} = \lambda/2$. This defines

\mathbf{H}_{mux} configuration and the locations of the D paths are illustrated in Fig. 3(b) which shows a contour plot of Ψ_{mux} . The corresponding AoA's/DoA's in the θ domain are generated for $\mathbf{H}_{v,bf}$ and \mathbf{H}_{id} using (9), Rem. 3 and $\theta = d \sin(\phi)/\lambda$. The contour plots of the resulting Ψ_{id} and Ψ_{bf} are shown in Figs. 3(c) and (d), and conform to the sizes of the non-vanishing sub-matrices $\tilde{\mathbf{H}}_v$ in Prop. 2; compare also with Fig. 2. As the transmit spacing d_t is decreased (with decreasing ρ), channel power is concentrated in fewer but larger non-vanishing transmit eigenvalues, as illustrated in Figs. 3(e)-(g). The capacities of the three configurations are estimated via 200 realizations of the scattering environment simulated using (2) by independently generating $\mathcal{CN}(0, 1)$ -distributed path gains. The estimated capacities corresponding to uniform-power input (Rem. 1) are plotted in Fig. 3(a) along with the theoretical curves (Fig. 1(b)) using (1). As evident, the agreement is quite remarkable.

4.1. Discussion

Reconfigurable MIMO transceivers can significantly enhance link capacity by delivering the maximum multiplexing gain (N) over the entire SNR range. The practical feasibility of reconfiguration in cognitive radio is enhanced by the fact that *three* canonical configurations suffice for near-optimal performance over the entire SNR range. Furthermore, only statistical channel state information (CSI) is needed: an estimate of the number of dominant virtual channel coefficients, D , with significant power. Once the receiver has estimated D , it can simply feedback to the transmitter the index of the optimal configuration at the desired SNR ($\log_2(3)$ bits of information).

In the context of cognitive radio and dynamic spectrum access, reconfigurable MIMO transceivers deliver the well-known capacity/spectral efficiency gains of MIMO systems at all SNR's, in contrast to a fixed configuration that only guarantees it at high SNR's. This directly leads to: i) N -fold reduction in transmission power at any desired rate, thereby significantly reducing interference to other users, and ii) N -fold increase in the information capacity of the available "holes" in RF spectrum.

Directions for future work include: i) extensions to more-realistic scenarios where the dominant scattering paths are non-uniformly distributed over the angular spreads, ii) extensions to wideband MIMO transceivers where the effects of multipath sparsity become even more pronounced, iii) exploiting instantaneous CSI (rather than statistical) with limited-rate feedback, and iv) optimization of reconfigurable MIMO links in a network context (accounting for effects of interference). In particular, limited-rate instantaneous CSI at the transmitter could significantly enhance interference management.

5. REFERENCES

- [1] A. M. Sayeed, "Deconstructing Multi-Antenna Fading Channels," *IEEE Trans. Sig. Processing*, pp. 2563-2579, Oct. 2002.
- [2] Y. Zhou, M. Herdin, A. M. Sayeed, and E. Bonek, "Experimental Study of MIMO Channel Statistics and Capacity via the Virtual Channel Representation," *to be submitted*.
- [3] V. Veeravalli, Y. Liang, and A. Sayeed, "Correlated MIMO Rayleigh Fading Channels: Capacity, Optimal Signaling and Asymptotics," *IEEE Trans. Inf. Th.*, pp. 2058-2072, June 2005.
- [4] A. Sayeed and V. Raghavan, "Maximizing MIMO Capacity in Sparse Multipath with Reconfigurable Antenna Arrays," *to appear in the IEEE J. Select. Topics Signal Processing*, 2007. Available online at <http://dune.ece.wisc.edu>.
- [5] S. Verdú, "Spectral Efficiency in the Wideband Regime," *IEEE Trans. Inf. Th.*, vol. 48, no. 6, pp. 1319-1343, June 2002.